

Structural control of building frames subjected to earthquake-induced excitations using shape memory alloys

Madan Alok¹ and Gupta Vimal Kumar^{2,*}

¹Department of Civil Engineering, Indian Institute of Technology Delhi, New Delhi 110 016, India

²Department of Civil Engineering, Hindustan College of Science and Technology, Farah, Mathura 281 122, India

The present article presents a concept for semi-active control of earthquake-induced vibrations in building frames based on smart stressing of the frames using shape memory alloys. Smart cables composed of nickel–titanium shape memory alloy wires are proposed to be installed externally with concrete building frame elements. Upon regulated electrical heating, the nickel–titanium shape memory alloy wires will undergo a martensite to austenite phase transformation resulting in large shrinkage strains. The strain energy thus induced can be used to generate significantly effective control forces in the building frame. The concept is analytically studied by numerical simulations of concrete building frames.

Keywords: Building frames, shape memory alloys, smart materials, structural control.

THE past two decades have witnessed intensive research activity in the area of vibration control in civil engineering structures^{1,2}. A number of innovative schemes and devices have been proposed for active, semi-active and passive control of vibrations in building structures. In recent years, the shape memory alloy (SMA)-based control systems have received growing interest in seismic protection of structures³. SMAs have also found successful applications in various engineering disciplines such as aerospace, mechanical and biomedical engineering. SMA is a smart material which exhibits two distinct attributes, i.e. the shape memory effect in its martensite phase and super-elasticity (SE) in its austenite phase, that are particularly desirable from the point of view of structural control.

A review of the literature shows quite a few research studies on application of SMAs for passive structural control⁴. Previously reported applications of SMA in structural base isolation include the implementation of SMA bars for base isolation of highway bridges⁵, SMA wire recentering devices for buildings⁶, SMA spring isolation systems^{7,8} and SMA tendon isolation system for a

multi-degree-of-freedom (MDOF) shear frame structure⁹. SMAs have been implemented as passive energy dissipation devices in braces for framed structures^{10–14}, in dampers for cable-stayed bridges¹⁵ and in connection elements for columns¹⁶. The literature review indicates limited research studies on active or semi-active structural control using SMAs^{17,18}. Most of the reported research focuses on application of SMAs for passive vibration control of structures, which takes advantage of only the damping property of super-elastic SMAs. The damping property of SMAs in their martensite phase and their unique shape memory effect, that offer considerable promise for SMAs to be utilized as dampers as well as actuators for semi-active and/or hybrid structural control, have received little attention thus far.

The present article presents an analytical study based on simulated semi-active structural control systems using smart cables composed of nickel–titanium (Ni–Ti) SMA wires that are externally installed in concrete building frames and can be electrically actuated to induce variable control forces for the reduction of seismic response of the frame. SMAs are materials that have the unique property to recover their shape after undergoing large deformations either through heating, i.e. the shape memory effect or by unloading, i.e. the super-elastic effect. The unique property is driven by a phase transformation between martensite and austenite phases. When Ni–Ti SMA in its parental phase (austenite) undergoes large deformations due to applied stresses produced by external loads, the deformations can be recovered or controlled by heating the material above the austenite finish temperature. Upon electrical heating, a martensite to austenite phase transformation takes place and the material undergoes large shrinkage strains. The strain energy thus induced can be used to actuate a substantial control force that can be varied by electrical heating, in principle, for semi-active vibration control of concrete building frames subjected to earthquake-induced ground excitation. The results of the present study indicate that the shape memory effect (SME) in Ni–Ti SMA is an effective mechanism for semi-active control of concrete building frames using smart cables constituted with SMA wires.

*For correspondence. (e-mail: vimalkumar.gupta.hcst@sgei.org)

Table 1. Mechanical properties of Nitinol¹⁹

Property	Ni–Ti shape memory alloys	
	Austenite	Martensite
Density (g/cm ³)	6.45	
Recoverable elongation (%)	up to 8	
Young's modulus (GPa)	30–83	21–41
Yield strength (MPa)	195–690	70–140
Ultimate tensile strength (MPa)	895–1900	
Elongation at failure (%)	5–50 (typically 25)	
Poisson's ratio	0.33	
Transformation temperature (°C)	–200–110°C	

Ni–Ti shape memory alloys

Ni–Ti SMA originally developed and termed as Nitinol by the US Department of Defense is a binary, equatomic inter-metallic (50% atomic Ni and 50% atomic Ti subjected to cold working and annealing treatment) compound of nickel and titanium. Owing to their higher ductility, larger recovery motion, super-elastic properties, superior resistance to corrosion and fatigue, stable transformation temperature and the intrinsic ability for shape recovery on heating, Nitinol alloys have the potential to emerge as suitable SMAs for practical applications in structural control devices.

Salient properties of Nitinol

The relevant mechanical properties of Ni–Ti SMAs are summarized in Table 1.

Stress–strain–temperature curve of Ni–Ti SMA

The unique attributes of SME and SE exhibited by Nitinol SMAs are manifested by a phase transformation between a crystallographic high-symmetry cubic crystal structure austenitic phase to a low-symmetry monoclinic crystal structure martensitic phase. Typically, martensite is stable at low temperatures and high stress values, whereas austenite is stable at high temperatures and low stress values. Figure 1 shows the mechanical behaviour of Ni–Ti SMA as a function of stress, strain and temperature¹⁹. Below the martensite finish temperature, M_f , SMA exhibits the shape memory effect. Deformations due to an applied stress are recovered by heating the material above the austenite finish temperature, A_f . At a temperature above A_f , SMA is in its parent phase, austenite. Upon reloading, stress-induced martensite is formed. Upon unloading, however, the material reverts to austenite at a lower stress, thereby resulting in the super-elastic behaviour. The nonlinear stress–strain relationship due to loading, unloading and reloading results in a hysteretic behaviour that is characteristic of Ni–Ti SMAs. In the context of the present study, the term ‘hysteresis’ signifies the non-single-valued stress–strain–temperature

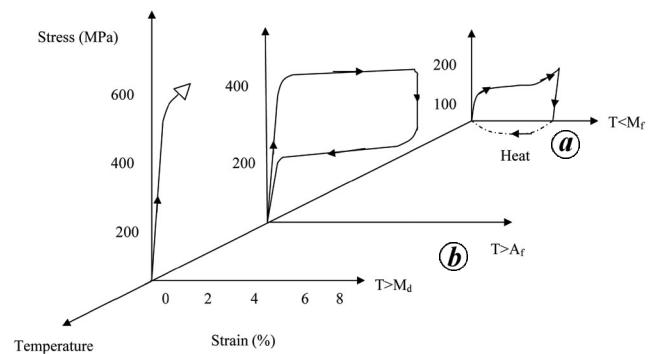


Figure 1. Stress–strain–temperature curve of Nitinol (Ni–Ti) shape memory alloy.

relationships for the Ni–Ti SMA. At a higher temperature above M_d ($T \gg A_f$), SMA undergoes ordinary plastic deformation with much higher strength. Thus, Ni–Ti SMAs display several characteristics that make them particularly amenable for applications in structural control. These characteristics include: (a) hysteretic damping, (b) large elastic strain range and related recentering capability, (c) excellent low and high-cycle fatigue resistance, (d) strain hardening at large strains and (e) a stress plateau, offering limited force transmission.

Hysteretic modelling of Ni–Ti SMA

The present study includes a modified form of the constitutive model for SMA initially developed by Graesser and Cozzarelli for modelling of the Ni–Ti SMA device. This model was extended by Wilde (Figure 2) and includes the hardening behaviour of SMA materials after transition from austenite to martensite phase is completed^{19,20}. The constitutive Wilde model describes the one-dimensional stress–strain relationship of super-elastic SMA wires. The modified Wilde model is of the form

$$\dot{\sigma} = E \left[\dot{\varepsilon} - |\dot{\varepsilon}| \left(\frac{\sigma - \beta}{Y} \right)^n \right] u_I(\varepsilon) + E_m \dot{\varepsilon} u_{II}(\varepsilon) + (3a_1 \dot{\varepsilon} \varepsilon^2 + 2a_2 \text{sign}(\varepsilon) \dot{\varepsilon} \varepsilon + a_3 \dot{\varepsilon}) u_{III}(\varepsilon), \quad (1)$$

$$\beta = E\alpha\{\varepsilon^{\text{in}} + f_T|\varepsilon|^c \text{erf}(a\varepsilon)[u(-\varepsilon\dot{\varepsilon})]\}, \quad (2)$$

where $\dot{\sigma}$, $\dot{\varepsilon}$, σ and β are slope of the stress–strain curve ($d\sigma/d\varepsilon$), rate of strain, stress and back stress respectively. The functions $u_I(\varepsilon)$, $u_{II}(\varepsilon)$ and $u_{III}(\varepsilon)$ are given by

$$u_I(\varepsilon) = (1 - u_{II}(\varepsilon) - u_{III}(\varepsilon)), \quad (3)$$

$$u_{II}(\varepsilon) = \begin{cases} 1 & |\varepsilon| \geq \varepsilon_m \\ 0 & \text{otherwise} \end{cases} \quad (4)$$

$$u_{III}(\varepsilon) = \begin{cases} 1 & \varepsilon\dot{\varepsilon} > 0 \text{ and } \varepsilon_1 < |\varepsilon| < \varepsilon_m \\ 0 & \text{otherwise} \end{cases}. \quad (5)$$

The term $E_m \dot{\varepsilon} u_{II}(\varepsilon)$ represents the elastic behaviour of martensite, which is activated when the strain is higher than ε_m . The strain value, ε_m defines the point when the transformation of SMA from austenite to martensite is completed. The smooth transition from the curve of slope E_y to slope E_m is obtained by adding the last term in eq. (1), which is evaluated only during loading and the strain $\varepsilon_1 < |\varepsilon| < \varepsilon_m$. The constants a_1 , a_2 and a_3 control the curvature of the transition. These are selected so that the slopes of the function defined by the last term at points ε_1 and ε_m are consistent with the slopes of plastic behaviour of SMA and martensitic elastic response. The smoothness of transition is governed by the selection of the slope at strain ε_2 .

Typical hysteretic parameters of Ni–Ti SMA

The following relevant characteristic material properties and hysteretic parameters were specified for simulation of Ni–Ti SMA in the present study.

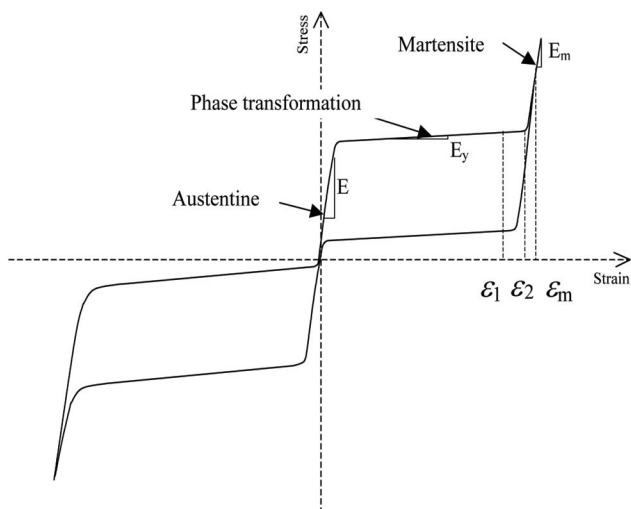


Figure 2. Stress–strain relation of the extended hysteretic model of Ni–Ti shape memory alloy.

Elastic modulus in austenite state, $E = 98.325$ GPa; yield stress, $Y = 144.9$ MPa; maximum strain in superelastic range, $\varepsilon_m = 0.08$; elastic modulus at martensite state, $E_m = 7.3744 \times 10$ MPa and elastic modulus during phase transformation, $E_y = \alpha E / (1 + \alpha)$; strain in the range of transition of pure martensite is given by $\varepsilon_1 = \text{strain} - 0.03$ and $\varepsilon_2 = (\varepsilon_m + \varepsilon_1) / 2.0$; the various constants controlling the shape of superelastic loop are given by

$$\alpha = 0.0197; n = 1; \omega = 1.0 \text{ rad/sec};$$

$$a = 900; c = 0.01; f_t = 0.08.$$

The values of a_1 , a_2 , and a_3 are derived as

$$a_1 = 124.844E_m + 199.75E_y,$$

$$a_2 = -0.344E_m - E_y,$$

$$a_3 = -0.90188E_m - 0.398E_y.$$

Figures 3 and 4 illustrate the super-elastic stress–strain and force–deformation behaviour of the Ni–Ti SMA

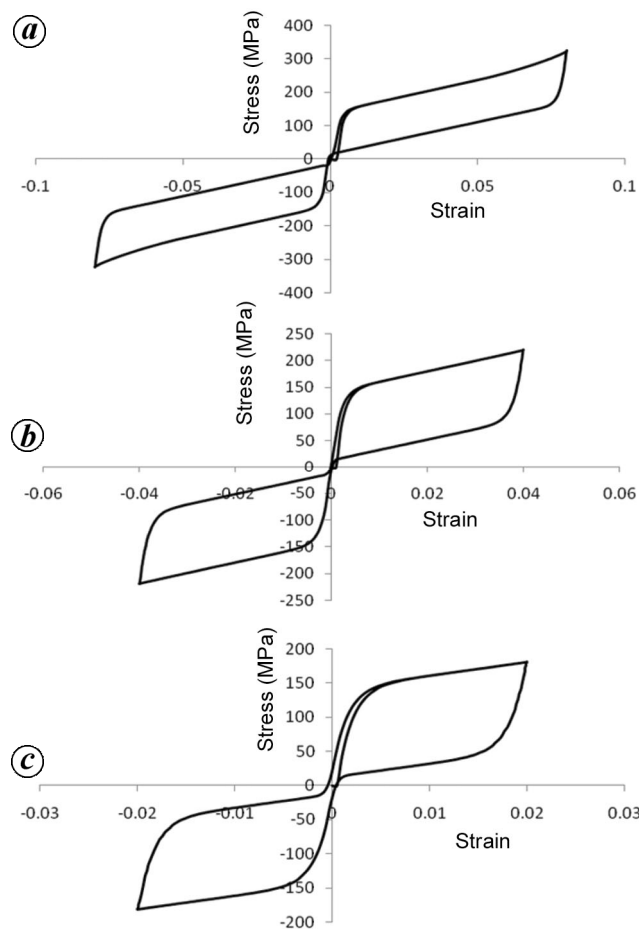


Figure 3. Stress–strain behaviour for Ni–Ti SMA wire at (a) 8%; (b) 4% and (c) 2% strain cycle.

wires derived from the modified Wilde model. These figures represent the solution of eqs (1) and (2). A MATLAB program was developed to employ the fourth-order Runge–Kutta forward integration along with the parameters defined above for the solution of the equations. The frequency of strain loading was taken as $\omega = 1$ rad/sec and time step = 0.025 sec was used in conjunction with 300 numerical integration steps for the cyclic response of three SMA models corresponding to different strain cycles of 2%, 4% and 8%. It may be best to use a combination of super-elastic and martensitic SMAs to exploit the characteristics of both damping and recentring and induce the required actuating force. Therefore, modified Wilde model of SMA semi-active tendons composed of Nitinol wires corresponding to 8% strain cycle was employed in the simulink model of building frame.

Semi-active control of building frames using Ni–Ti SMAs

In theory, the single degree-of-freedom (SDOF) frame can be considered as a mathematical model of a single-

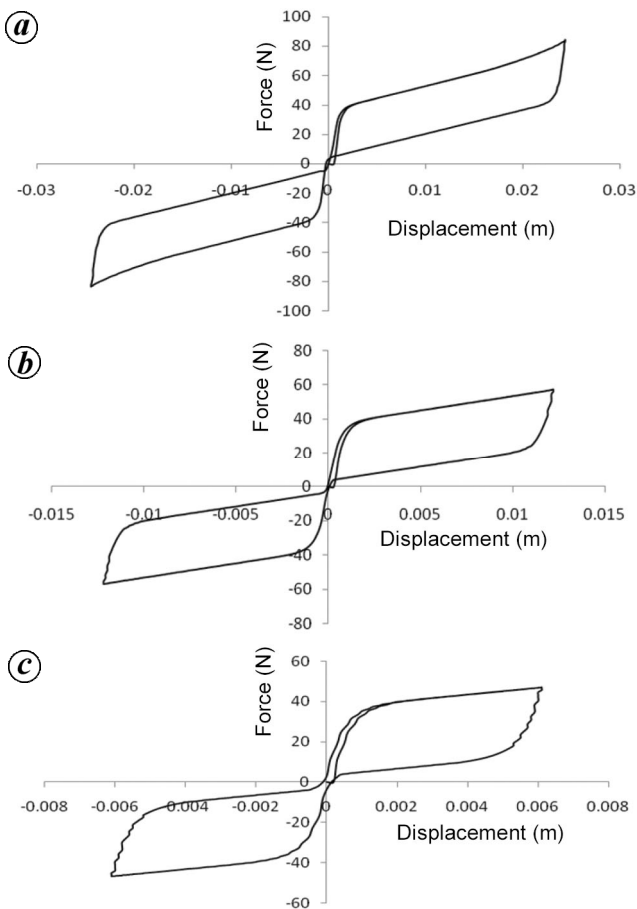


Figure 4. Force–displacement behaviour for Ni–Ti SMA wire at (a) 8%; (b) 4% and (c) 2% strain cycle.

storey concrete building frame with the idealized semi-active tendons representing the smart stressing cables composed of Nitinol SMA wires that are installed in a building frame. In practice, the smart cables need to be designed, detailed and implemented in the concrete building frame to achieve the theoretically desired and predicted semi-active control of the actual building frame. It should be mentioned here that the practical implementation issues of the proposed semi-active control technique using smart cables composed of SMAs are beyond the scope of the present study. In principle, however, the Ni–Ti SMA wires that constitute the smart cables for semi-active control of the idealized SDOF frame model have the unique ability to recover their shape after undergoing large deformations at a given temperature either by heating or removal of the external load.

Design considerations for semi-active tendons

The semi-active control force can be actuated by electrical heating of the Ni–Ti SMA wires comprising the semi-active tendons by a design pulsed current. For the purpose of design, a modified version of the analytical model proposed by Wilde *et al.*⁵ for the hysteretic stress–strain relationship of super-elastic Ni–Ti SMA wires may be employed for predicting the hysteretic force–displacement behaviour of these wires. Practically, the semi-active tendon would comprise of a large number of SMA wires whose numbers are assessed on the basis of maximum control force required during the entire duration of the earthquake ground motion. Theoretically, the control force can be altered based on feedback from sensors for closed loop control by actuating a specified number of SMA wires using electrical heating at constant temperature.

The composition and properties of Nitinol SMA wires that constitute the smart cables are:

Percentage of Ni by weight = 55.32; percentage of Ti by weight = 44.68; martensite finish temperature, $M_f = 24.6^\circ\text{C}$; martensite start temperature, $M_s = 40.2^\circ\text{C}$; austenite start temperature, $A_s = 53.7^\circ\text{C}$; austenite finish temperature, $A_f = 74.4^\circ\text{C}$, and diameter of Nitinol wire = 0.6 mm.

As an actuator, Nitinol wire of 0.6 mm diameter and 308 mm length is capable of developing internal restoration stresses of around 170 MPa at 4% strain. An electric current of 4.91 A generates sufficient heat to trigger the required phase transformation. The force induced over the cross section of the wire can be calculated as

$$F = 170 \times (\pi/4) \times (0.6)^2 = 48 \text{ N.}$$

Theoretically, therefore, a single Ni–Ti SMA wire (length = 308 mm and diameter = 0.6 mm) can actuate a force of 48 N at 4% strain.

Control algorithm

Consider a multi degree-of-freedom (MDOF) structure with n degrees of freedom, subjected to earthquake ground acceleration \ddot{x}_g . Assuming that the control forces f are adequate to keep the entire structure within the elastic range, the equation of motion is given by

$$M\ddot{X} + C\dot{X} + KX = df - M\ddot{x}_g, \tag{6}$$

where X is the vector of relative displacement; f a vector of control force corresponding to n_c number of dampers; M , C and K are mass, damping and stiffness matrices of appropriate size d representing an $n \times n_c$ location matrix denoting the control force location on the structure due to location of SMA dampers, and I is a vector of unity. The state-space form of the equation of motion is given by

$$\dot{z} = Az + Bf + E_c\ddot{x}_g \quad y = C_o x + D_o,$$

$$A = \begin{bmatrix} 0 & I \\ -M^{-1}K & -M^{-1}C \end{bmatrix}, \quad B = \begin{bmatrix} 0 \\ M^{-1}d \end{bmatrix},$$

and $E_c = \begin{bmatrix} 0 \\ -1 \end{bmatrix}$, (7)

where A is a $2n \times 2n$ system matrix, B a $2n \times n_c$ control matrix, E_c a $2n \times 1$ location matrix of the excitation, z a $2n \times 1$ state vector, y the measured output, C_o and D_o are the output matrices.

The bang–bang type controller has been implemented in the Simulink model of MATLAB, using an integration time step of 0.02 sec. The structural model is incorporated with the help of the state space block of Simulink. For the present SMA device, the control strategy is given by

$$f = \begin{cases} f_a & \text{strain} \leq 4.0\%, \\ f_{\max} & \text{otherwise,} \end{cases} \tag{6}$$

where f is the control force of the SMA device, f_a the desired control force which is obtained by the classical optimal as primary controller and f_{\max} is the maximum capacity of the semi-active control device. For a given state, the desired control force and corresponding current for actuation of SMA wires are obtained.

Case studies for numerical simulation of SMA-based semi-active control

Two numerical examples were simulated for theoretical evaluation of the efficacy of the proposed semi-active control technique using Ni–Ti SMAs.

Example 1 – Single-storey frame model with SMA-based semi-active tendons

The dynamic parameters of SDOF model were assumed as: mass, $m = 29,485$ kg; stiffness, $k = 11,912$ kN/m and damping coefficient, $c = 23.71$ kN-s/m. The structural frame model was subjected to the El Centro earthquake ground motion depicted in Figure 5. Simulation of the idealized structural control system was performed using the Simulink toolbox in MATLAB. The flowchart of the simulation is illustrated using the block diagram approach in Figure 6. The feedback variables $x(t)$ and $\dot{x}(t)$ for closed-loop control were assumed to be sampled at an interval of 0.02 sec. A time instant of 0.02 sec was used to calculate the instantaneous control force to be induced in the semi-active tendon. The closed-loop control force was calculated using a simplistic control algorithm described earlier.

Example 2 – Eight-storey frame model with multiple SMA-based semi-active tendon systems

An eight-storey frame model was considered for numerical simulation of the proposed semi-active control scheme

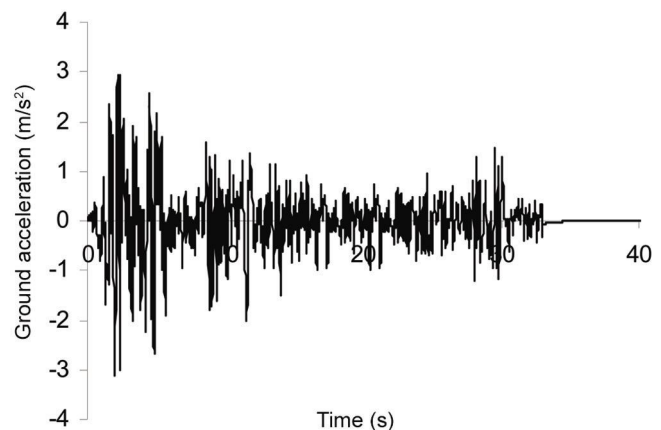


Figure 5. El Centro earthquake ground motion.

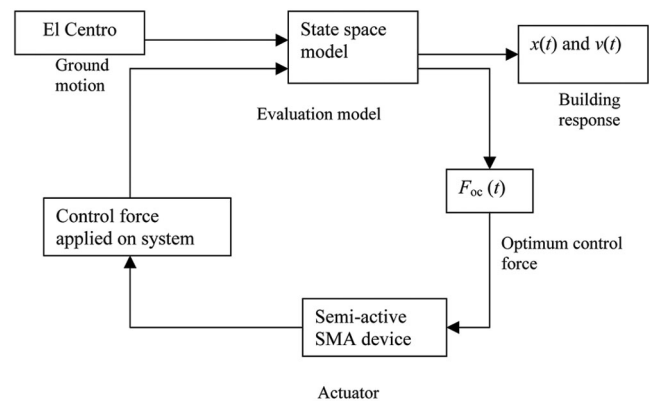


Figure 6. Flow chart using block diagram approach for simulation of structural control system.

Table 2. Response reduction in single-storey frame model controlled with semi-active tendons composed of Nitinol shape memory alloy (SMA) wires

Control system	Maximum displacement (m)	Maximum velocity (m/s)	Maximum control force (kN)
Uncontrolled frame	0.0262	0.56	–
Single-storey frame with SMA-based semi-active tendons	0.0136	0.29	59.4

Table 3. Comparison of dynamic response and control force parameters for the eight-storey frame model with SMA-based semi-active tendons²

Control system	Maximum displacement at top floor (m)	Maximum velocity at top floor (m/s)	Maximum control force (kN)				Total
			Floor no.				
			I/II	III/II	V/III	VII/IV	
Uncontrolled	0.171	1.06	–	–	–	–	–
Frame with SMA-based semi-active tendons at floors 1, 3, 5, 7	0.0627	0.57	74	214	327	398	1013
Frame with SMA-based semi-active tendons at floors 1–4	0.0819	0.68	121	239	350	450	1161
Frame with active mass driver on the roof	0.0431	0.3912	–	–	–	–	1774

using SMAs in MDOF structures². The proposed semi-active tendons constituted with Ni–Ti SMA wires were assumed to be implemented in alternate floors (storeys 1, 3, 5 and 7) as well as lower consecutive floors (storeys 1–4) for investigation of the control performance. The dynamic structural parameters specified for the originally reported model were floor mass, $m = 245.6$ tonnes; lateral stiffness of each storey $k = 3.404 \times 10^5$ kN/m and viscous (natural) damping constant of each storey, $c = 2937$ tonnes/sec, which corresponds to a 2% damping ratio for the first vibration mode of the entire structure. The angle of inclination of the semi-active tendons with respect to the horizontal is 60° . The computed natural frequencies for the MDOF structural model are 5.79, 17.18, 27.98, 37.82, 46.38, 53.36, 58.53 and 61.69 rad/sec. The Simulink model was developed in MATLAB for simulation of the structural control system using SMA-based semi-active tendons. The closed-loop control forces in the semi-active tendons were computed using the control algorithm explained earlier.

Results of simulated case studies

SDOF single-storey frame model

Comparison of the simulated dynamic time-histories of displacement for the single-storey frame model with SMA-based semi-active tendons with the uncontrolled dynamic response of the frame model under the action of the El Centro earthquake ground motion is illustrated in Figure 5. The number of SMA wires that need to be actuated will vary with the computed control force as

assessed by the control algorithm of the system. Table 2 summarizes the peak values of the dynamic response and control force for the single-storey frame model with SMA-based semi-active tendons in contrast to the uncontrolled frame.

MDOF eight-storey building frame model

Comparison of peak values of the dynamic response and control parameters for the eight-storey frame model with SMA-based semi-active tendons installed at alternate floors (1, 3, 5, 7), consecutive floors (1–4) versus the corresponding uncontrolled frame is given in Table 3. The table also includes the peak displacement response and control force for the originally reported multi-storey frame model with an active mass driver (AMD) installed on the roof. An alternative arrangement of the SMA-based semi-active tendon system with the tendons located at lower consecutive floors 1–4 was also investigated in the present study. The peak values of the response and control force for the alternative arrangement are also included in Table 3.

Conclusions

The present study is based on a theoretical investigation of semi-active control of concrete building frames using smart stressing cables composed of Ni–Ti SMA wires that are externally installed in the building frames and can be electrically actuated to induce variable control forces for controlling the seismic response of the frame. The results of the present study indicate that the shape

memory effect and super-elasticity in Ni–Ti SMAs are an effective mechanism for semi-active control of concrete building frames using smart cables constituted with SMA wires. The results of mathematical modelling and numerical simulation of the buildings frame with the smart cables idealized as semi-active tendons composed of Nitinol SMA wires point to the following specific conclusions:

(1) The proposed semi-active control technique implementing the SMA-based tendons is distinctly effective in the response reduction of the building frame. Displacement is reduced by 63.3% and 52.1% for the tendons are placed at odd floors 1, 3, 5, 7 and at consecutive floors 1–4 respectively, compared to the reduction of 74.7% in the case of AMD on the top floor. Similarly, the velocity is reduced by 46.22% and 35.85% for the tendons placed at odd floors 1, 3, 5, 7 and at consecutive floors 1–4 respectively, compared to 63.1% in the case of AMD on the top floor.

(2) The proposed control algorithm is simple and straightforward in terms of implementation. It requires only judicious selection of the number of wires to be actuated by electrical heating to induce the required control force.

(3) The arrangement of Ni–Ti SMA-based semi-active tendon controllers at the alternate floors results in superior control effectiveness in comparison to placement at lower consecutive floors. It reduces the displacement by 0.0627 m compared to 0.0819 m in case of tendon controllers at consecutive floors from the bottom.

(4) The response reduction resulting from the SMA-based semi-active control and the benchmark active mass driver is comparable and proportionate to the applied control force.

1. Housner, G. W., Structural control: past, present and future. *J. Eng. Mech.*, 1997, **123**(9), 897–971.
2. Soong, T. T., *Active Structural Control Theory and Practices*, Longman Scientific & Technical, 1991.
3. Yunfeng, Z. and Songye, Z., Seismic response control of structures with superelastic shape memory alloy wire dampers. *J. Eng. Mech.*, 2008, **134**(3), 240–251.
4. Song, G., Ma, N. and Li, H. N., Applications of shape memory alloys in civil structures. *J. Eng. Struct.*, 2006, **28**, 1266–1274.
5. Wilde, K., Gardoni, P. and Fujino, Y., Base isolation system with shape memory alloy device for elevated highway bridges. *Eng. Struct.*, 2000, **22**(3), 222–229.

6. Dolce, M., Cardone, D. and Marnetto, R., SMA re-centering devices for seismic isolation of civil structures. *Proc. SPIE*, 2001, **4330**, 238–249.
7. Khan, M. M. and Lagoudas, D., Modelling of shape memory alloy pseudoelastic spring elements using Preisach model for passive vibration isolation. *Proc. SPIE*, 2002, **4693**, 336–347.
8. Mayes, J. J., Lagoudas, D. and Henderson, B. K., An experimental investigation of shape memory alloy pseudoelastic springs for passive vibration isolation. In AIAA Space 2001 Conference and Exposition 4569, NM, USA, 2001.
9. Crobi, O., Shape memory alloys and their application in structural oscillations attenuation. *Simul. Model. Practice Theory*, 2003, **11**, 387–402.
10. Clark, P. W., Aiken, I. D., Kelly, J. M. and Krumme, R. C., Experimental and analytical studies of shape memory alloy dampers for structural control. *Proc. Passive Damping, SPIE*, 1995, **2445**, 241–251.
11. Dolce, M., Cardone, D. and Marnetto, R., Implementation and testing of passive control devices based on shape memory alloys. *Earthquake Eng. Struct. Dyn.*, 2000, **29**(7), 945–968.
12. Han, Y. L., Li, Q. S., Li, A. Q., Leung, A. Y. T. and Lin, P. H., Structural vibration control by shape memory alloy damper. *Earthquake Eng. Struct. Dyn.*, 2003, **32**, 483–494.
13. Ma, N., Song, G. and Tarefder, R. A., Vibration control of a frame structure using shape memory alloy braces. In Proceedings of Third International Conference on Earthquake Engineering, China, 2004, pp. 223–235.
14. Saadat, S., Noori, M., Davoodi, H., Zhou, Z., Suzuki, Y. and Masuda, A., Using NiTi SMA tendons for vibration control of coastal structures. *Smart Mater. Struct.*, 2001, **10**, 695–704.
15. Li, H., Liu, M. and Ou, J. P., Vibration mitigation of a stay cable with one shape memory alloy damper. *Struct. Control Health Monit.*, 2004, **11**, 21–36.
16. Tamai, H. and Kitagawa, Y., Pseudoelastic behaviour of shape memory alloy wires and its application to seismic resistance member for building. *Comput. Mater. Sci.*, 2002, **25**, 218–227.
17. McGravin, G. and Guerin, G., Real time seismic damping and frequency control of steel structures using Nitinol wires. *Proc. SPIE*, 2002, **4696**, 176–184.
18. Mo, Y. L., Song, G. and Otero, K., Development and testing of a proof-of-concept smart concrete structure. In Proceeding of Smart Structures Technologies and Earthquake Engineering, Osaka, Japan, 2004.
19. DesRoches, R., McCormick, J. and Delemont, M., Cyclic properties of superelastic shape memory alloy wires and bars. *J. Struct. Eng.*, 2004, **130**, 38–46.
20. Graesser, E. J. and Cozzarelli, F. A., Shape memory alloys as new materials for aseismic isolation. *J. Eng. Mech.*, 1991, **117**(11), 2590–2608.

Received 30 March 2014; revised accepted 21 August 2014